Supplementary Information for:

Alternate InP Synthesis with Aminophosphines: Solution-Liquid-Solid Nanowire Growth

Helen C. Larson,[1] Zhixing Lin,[2] François Baneyx,[2] Brandi M. Cossairt*[1]

[1]Department of Chemistry, University of Washington, Seattle, WA 98195, USA

[2]Department of Chemical Engineering, University of Washington, Seattle, WA 98195, USA

*cossairt@uw.edu

Sections:

1. Experimental Methods

General Practices

All glassware was dried in a 160 °C oven overnight prior to use. All syntheses were performed under an inert atmosphere of nitrogen using a glovebox or standard Schlenk techniques. Indium chloride (98%) and indium metal pieces (99.99% trace metals basis) were purchased from MilliporeSigma and dried under vacuum before being stored in a nitrogen glovebox. Oleylamine (≥98%) and diethylamine (≥99.5%) were purchased from MilliporeSigma, dried over CaH_2, distilled, and stored over activated 3 Å molecular sieves in a nitrogen glovebox. Toluene-d_8 (99.5%) were purchased from Cambridge Isotope Laboratories and was similarly dried and stored. Anhydrous tris(diethyl)aminophosphine (97%), phosphorus(V) oxychloride (99%), trifluoroacetic acid (99%), and anhydrous methanol (99.8%) were purchased from MilliporeSigma and used without further purification. Trifluoroacetic anhydride (>98.0%) was purchased from TCI America and used without further purification. Indium(III) iodide (99.999%) and indium(III) trifluoromethanesulfonate (99%) were purchased air-free from Strem Chemicals, Inc. and used without further purification. Toluene (high-performance liquid chromatography grade) was purchased from Fisher and used as purchased for UV-vis absorbance spectroscopy of reaction aliquots. High-performance liquid chromatography grade toluene (used for purifications), dichloromethane, and tetrahydrofuran were purified and dried using a solvent still[1], and stored over activated 3 Å molecular sieves in a nitrogen glovebox. For use in electrochemistry, benzonitrile (>99.0%) was purchased from TCI and dried over phosphorous pentoxide then fractionally vacuum distilled (discarding the first and last 5%). The drying and distillation was repeated. Tetrabutylammonium hexafluorophosphate ([TBA][PF6], 98%) was purchased from VWR Scientific and recrystallized twice from ethanol. UV-vis spectra were collected on a Cary 5000 spectrophotometer from Agilent.

Synthesis of In(trifluoroacetate)$_3$

Adapted from a reported synthesis of $In(TFA)_3$.[2] In a nitrogen glovebox, 6 mmol (1 equivalent) indium metal and 9 equivalents trifluoroacetic acid were added to a 50 mL Schlenk flask equipped with a stir bar and sealed with a septum. The reaction was then placed under nitrogen on the Schlenk line with a reflux condenser and was heated until reflux and held overnight yielding a fine white powder and excess trifluoroacetic acid. The excess acid was removed under vacuum. In a nitrogen glovebox, the white powder was washed with pentanes or hexanes and dried under vacuum. ^{19}F (470 MHz, toluene-d_8, 270 K): δ -75.81. ESI-MS *m/z*: $[[In(O_2CCF_3)_4]_2]^{2-}$ calcd for C16F24In2O16 566.8, found 566.7. $[In(O_2CCF_3)_2[HOCH_3]_2]^+$ calcd for C6H8F6In1O6 404.9, found 404.8.

Synthesis of InP Nanowires using In(trifluoroacetate)$_3$

Adapted from aminophosphine-based InP QD synthesis conditions.[3] In a nitrogen glovebox, 0.3 mmol $In(TFA)_3$ and 5 mL anhydrous oleylamine were added to a 50 mL 3-neck flask equipped with a stir bar. On the Schlenk line, the solution was placed under vacuum at 120 °C and degassed for 1 h, with 300 rpm stirring. The vessel was then placed under an inert atmosphere and heated to 180 °C. Once the reaction temperature was reached, 0.33 mL of

tris(diethyl)aminophosphine (1.2 mmol) was rapidly injected. If multipods form instead of nanowires, increase the tris(diethyl)aminophosphine injection to 0.36 mL (1.32 mmol). The reaction was monitored by UV-vis absorbance spectroscopy of 20 μL reaction aliquots in 2 mL toluene. The reaction was allowed to proceed overnight for approx. 20 hr. The flask was then cooled down to room temperature before being moved into a nitrogen glovebox for purification. The nanowires were collected by centrifugation of the crude reaction solution for 10 min at 7830 rpm, and resuspended in 2-3 mL toluene. The nanowires were washed with toluene this way 3 times to remove excess oleylamine and the quantum dot coproduct before further characterization. The quantum dot product remained in the supernatant and was separately precipitated with anhydrous methanol, centrifuged for 10 min at 7830 rpm, and resuspended in toluene. This procedure was repeated 3 times to remove excess oleylamine before additional sample analysis was performed.

Synthesis of InP Nanowires using In(trifluoromethanesulfonate)$_3$

InP nanowires were synthesized using the same procedure as above but instead of 0.3 mmol $In(TFA)_3$, 0.3 mmol of $In(OTf)_3$ was used, and the reaction was allowed to proceed until the absorbance spectrum remained constant, observed after 2 hours of reaction.

Synthesis of InP Nanowires using External In^0 Nanoparticles

The indium nanoparticles were synthesized following a literature synthesis.[4,5] The synthesis of InP nanowires including indium nanoparticles in addition to $In(TFA)_3$ was ran similar to above except 0.1 mL of a 0.008 M solution of indium nanoparticles in oleylamine was injected alongside the aminophosphine.[6] The synthesis of InP nanowires including indium nanoparticles without $In(TFA)_3$ was ran as follows: 4.5 mL oleylamine was added to a 50 mL 3-neck flask under nitrogen on the Schlenk line and heated to 180 °C. Once the reaction temperature was reached, 0.33 mL of tris(diethylamino)phosphine (1.2 mmol) was rapidly injected, immediately followed by a rapid injection of a solution of 0.0449 g indium nanoparticles (0.3 mmol indium atoms) in 0.5 mL oleylamine. The reaction proceeds and was purified similar to above.

Control Synthesis without Aminophosphine

The reaction of indium tris(trifluoroacetate) and oleylamine was ran similar to the synthesis of InP nanowires using indium tris(trifluoroacetate) above, except without the hot injection of aminophosphine.

Control Synthesis with Diethylamine

The reaction of indium tris(trifluoroacetate), oleylamine, and diethylamine was ran similar to the synthesis of InP nanowires using indium tris(trifluoroacetate) above, except in a closed system to avoid rapid evaporative loss of diethylamine. In a nitrogen glovebox, 0.06 mmol $In(TFA)_3$ (0.0272 g, 1 eq.) and 1 mL oleylamine (3 mmol, 51 eq.) was added to a 15 mL 3-neck flask equipped with a t-adapter and stopper. The flask was placed under vacuum at 120 °C and degassed for 1 h. Then, the flask was placed back under nitrogen, cooled to room temperature, and brought into the glovebox. 74.4 microliters of diethylamine was added, and the solution was transferred to a J. Young tube. Heat the solution at 180 °C for 2 hours in a silicone oil bath. The

reaction was then cooled down to room temperature before being moved into a nitrogen glovebox for purification similar to the nanowire synthesis.

Synthesis of Tris(oleylamino)phosphine oxide

Tris(diethylamino)phosphine oxide was synthesized by adapting a literature procedure for tris(dimethylamino)phosphine oxide by substituting dimethylamine for diethylamine.[7] ^{1}H (500 MHz, toluene-d_8); δ 2.91 (dq, $J_{H\text{-}P}$ = 14.1 Hz, $J_{H\text{-}H}$ = 7.1 Hz, 12 H), 0.91 (t, $J_{H\text{-}H}$ = 7.1 Hz, 18 H). ^{31}P {H} (202 MHz, toluene-d_8); δ 26.68. Then, the tris(diethylamino)phosphine was transaminated by adapting previous literature methods.[8,9] One equivalent of tris(diethylamino)phosphine was heated under nitrogen at 120 °C for two hours with 5 equivalents of oleylamine to produce tris(oleylamine)phosphine. ^{31}P {H} (202 MHz, toluene-d_8); δ 20.50.

^{19}F NMR Study of Trifluoroacetic Anhydride

N-oleyltrifluoroacetamide was synthesized by mixing 6.3 μL of trifluoroacetic anhydride (0.045 mmol, 1.5 eq.) and 0.5 mL oleylamine (1.52 mmol, 51 eq) in a nitrogen glovebox in an oven-dried J. Young tube. The reaction was heated to 180 °C in a silicone oil bath for 1 hour, and characterized by ^{19}F NMR spectroscopy.

Synthesis of InP Quantum Dots from InI_3 or $InCl_3$

InP QDs made from InI_3 or $InCl_3$ were synthesized as described previously in literature.[10] The insoluble reaction product was collected by centrifugation of the crude reaction solution for 10 min at 7830 rpm for characterization by PXRD.

Transmission Electron Microscopy (TEM)

All TEM imaging was done on a FEI Tecnai G2 F20 SuperTwin microscope operated at 200 kV using bright field, HAADF STEM, and Elite T EDAX EDS modes. Samples were prepared in a nitrogen glovebox by drop-casting 5 μL of dilute suspensions in toluene onto a suspended ultrathin carbon film on a lacey carbon support film, 400 mesh, copper grids purchased from Ted Pella Inc, and allowed to dry fully (10 min) then placed under vacuum overnight. TEM size analysis was performed using manual analysis in ImageJ based off images from at least two different grid locations and over 300 diameter measurements per sample.

Scanning Electron Microscopy (SEM)

All SEM imaging was done on a ThermoFisher Scientific Apreo 1 SEM.

Atomic Force Microscopy (AFM)

All AFM images were collected using ScanAsyst-Air probes (Bruker, CA) in Peakforce Tapping mode with a Dimension Icon AFM (Bruker, CA) at room temperature. Images were analyzed using Nanoscope Analysis v1.5 (Bruker, CA).

Powder X-ray Diffraction (PXRD)

Powder XRD diffraction patterns were collected on solid films drop-cast onto a Si wafer using a Bruker D8 Discover diffractometer.

NMR Spectroscopy

^{1}H, ^{19}F, and ^{31}P NMR spectra were recorded on 500 MHz Bruker Advance spectrometers. Samples prepared for ^{19}F NMR spectroscopy included a sealed capillary of 0.01 M trifluorotoluene in toluene for reference in accordance to literature.[11] Samples prepared for ^{31}P NMR spectroscopy included a sealed capillary of 2 or 80 weight % H_3PO_4 in H_2O referenced to 0.72 or 0.00 ppm, respectively. Diffusion-ordered spectra were analyzed using Bruker's TopSpin software.

Mass Spectrometry

Mass spectra were recorded on a Bruker EsquireLC – Ion Trap Mass Spectrometer.

Cyclic Voltammetry

All electrochemical experiments were performed in a nitrogen-filled glove box. The potentiostat used was an EC Epsilon from BASi. Glassy carbon disk electrodes with a diameter of 3.0 mm were polished using 5, 1, and 0.1 micron polishing powder with sonication in ultrapure water between steps. The counter electrode was a platinum wire, and the pseudoreference electrode was a silver wire in a ceramic-fritted glass tube (Pine) filled with 0.1 M [TBA][PF_6].

Inductively Coupled Plasma – Optical Emission Spectrophotometry (ICP-OES)

ICP-OES of quantum dot samples was taken on a Perkin Elmer Optima 8300. QD solids were digested with H_2O_2 and nitric acid overnight and diluted with 18 MΩ water to prepare ICP samples.

2. Supplementary Figures (S1-S21)

a)

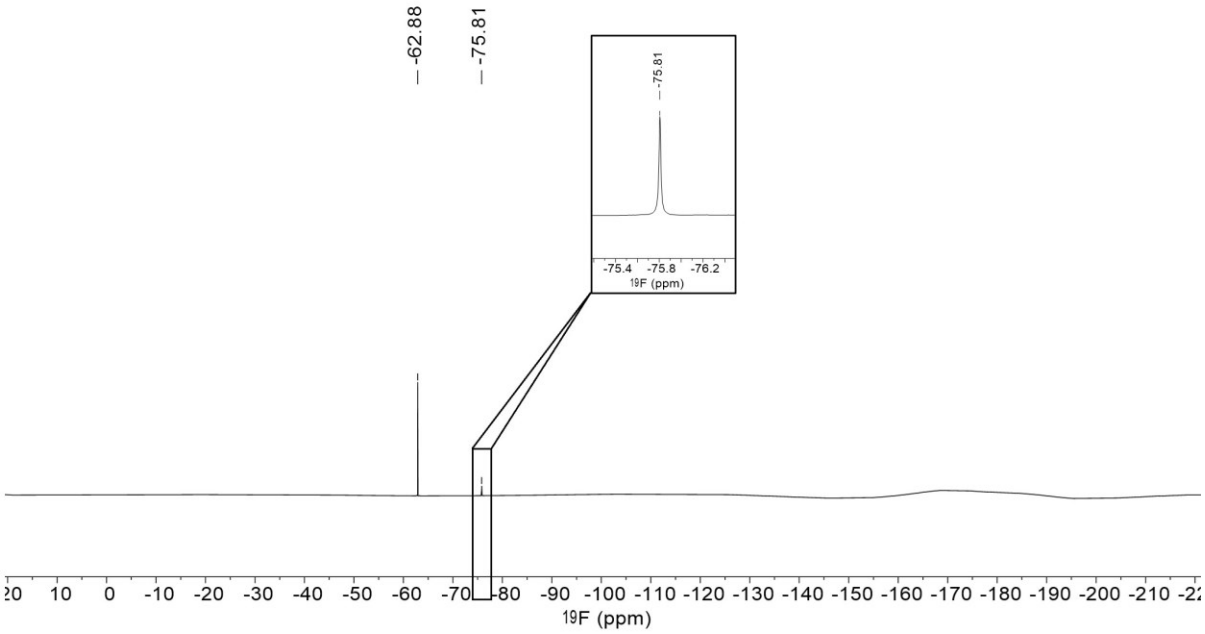

b)

Analysis Info

Analysis Nam	HelenB07.d	Acquisition D	01/04/24 15:14:11	Operator	Administrator
Sample Nam	Default	Method	Copy of XQ Default.ms	Instrument	Esquire-LC_00066
Comment	Negative 30-70 skim voltage				

Acquisition Parameter

Ion Source Type	ESI	Mass Range	Std/Normal	Ion Polarity	Negative	Alternating Ion	n/a
Scan Begin	50.00 m/z	Scan End	2200.00 m/z	Averages	4 Spectra	Polarity	
Capillary Exit	-100.0 Volt	Skim 1	-30.0 Volt	Trap Drive	55.0	Accumulation Time	198 µs
						Auto MS/MS	Off

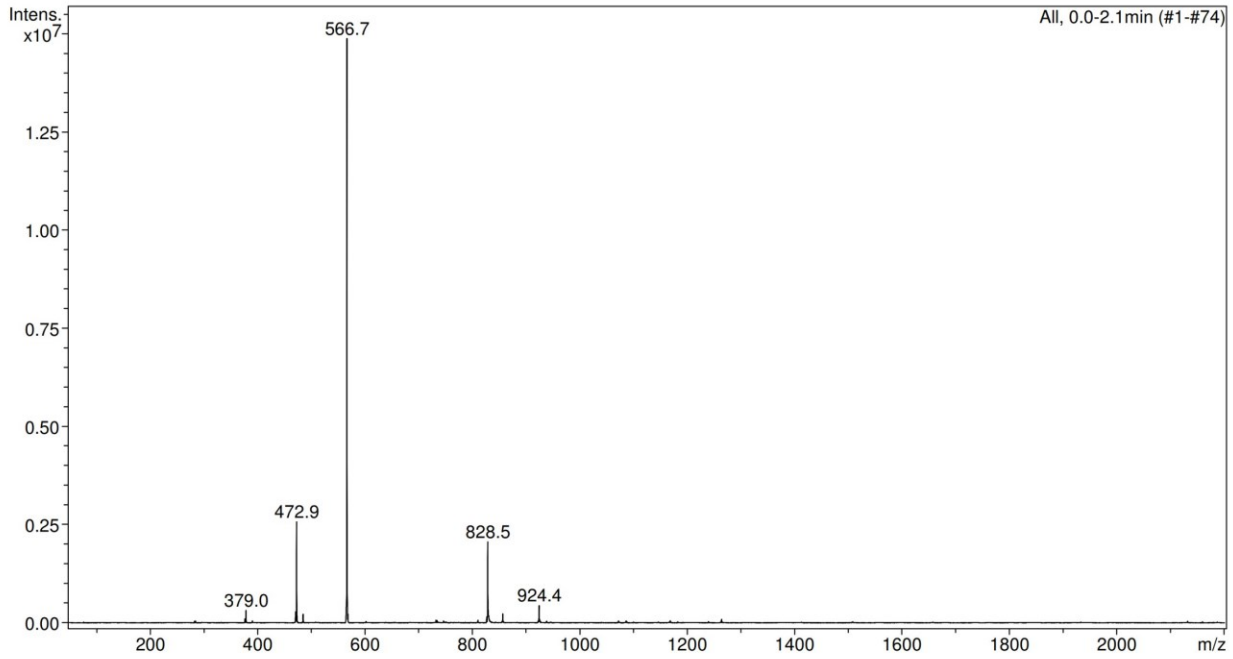

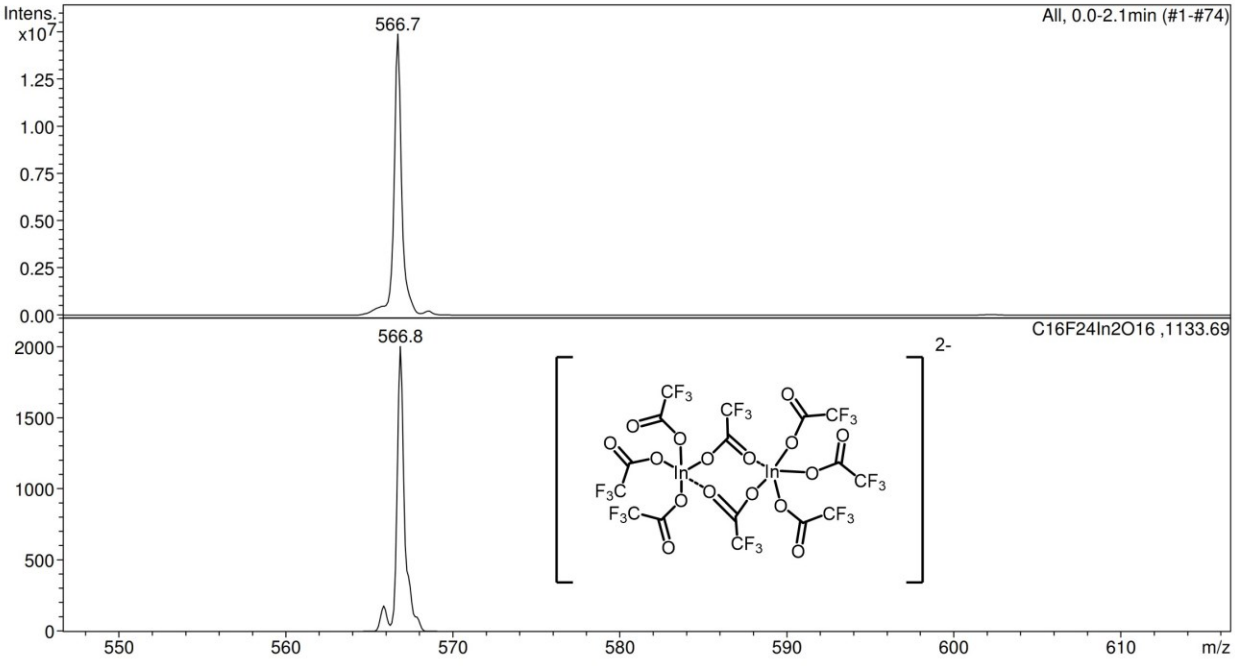

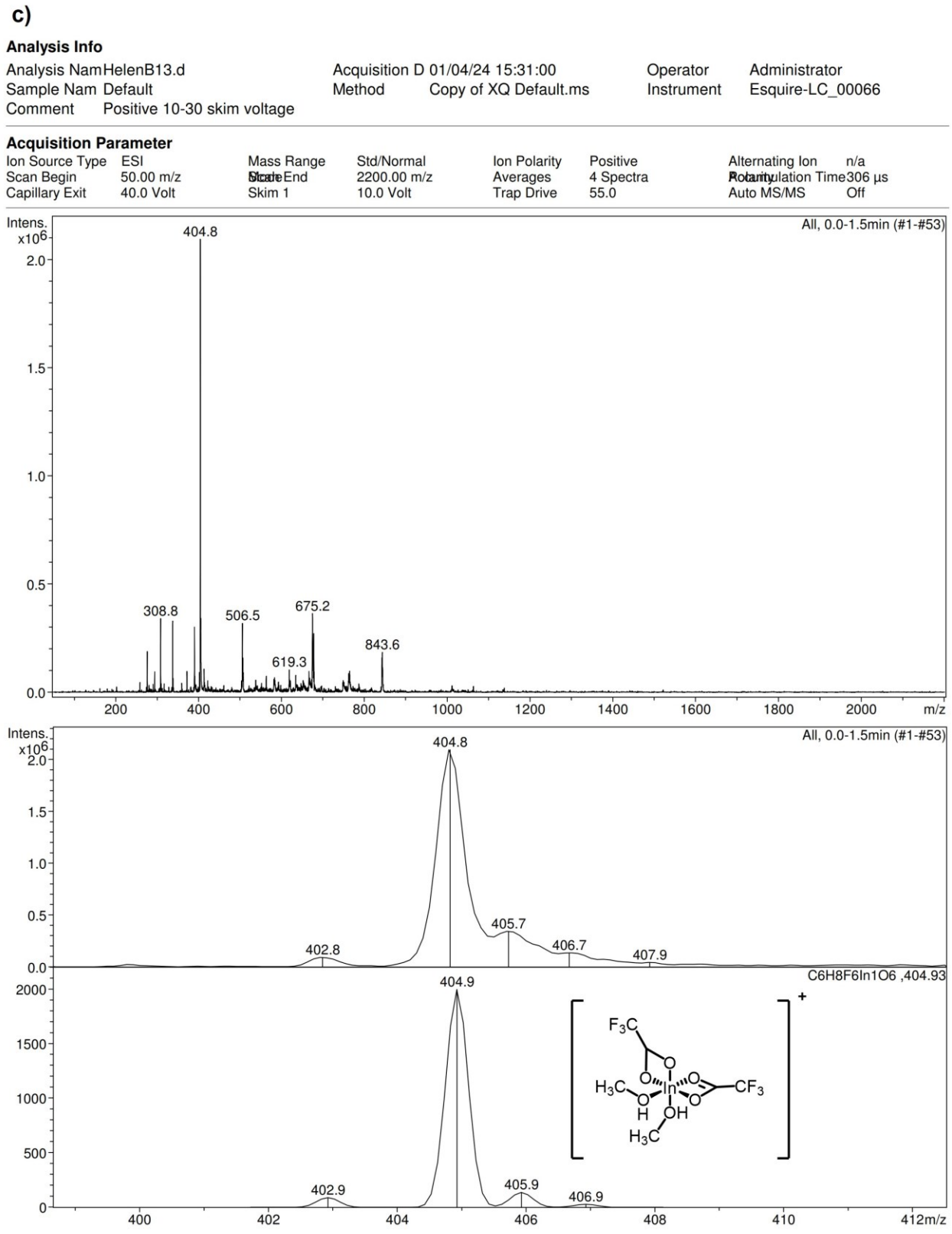

Figure S1. Characterization of $In(TFA)_3$. **a)** ^{19}F NMR spectrum of $In(TFA)_3$ (470 MHz, toluene-d_8, DS 2, NS 40, D1 10 s). **b)** Negative mode mass spectrum of $In(TFA)_3$ in methanol, with the

main fragment observed at 566.7 *m/z* matching the isotope pattern and molecular weight of the dimer $[[In(O_2CCF_3)_4]_2]^{2-}$, calculated for C16F24In2O16 at 566.8 *m/z*. **c)** Positive mode mass spectrum of $In(TFA)_3$ in methanol, with the main fragment at 404.8 *m/z* matching the isotope pattern and molecular weight of $[In(O_2CCF_3)_2[HOCH_3]_2]^+$, calculated for C6H8F6In1O6 at 404.9 *m/z*.

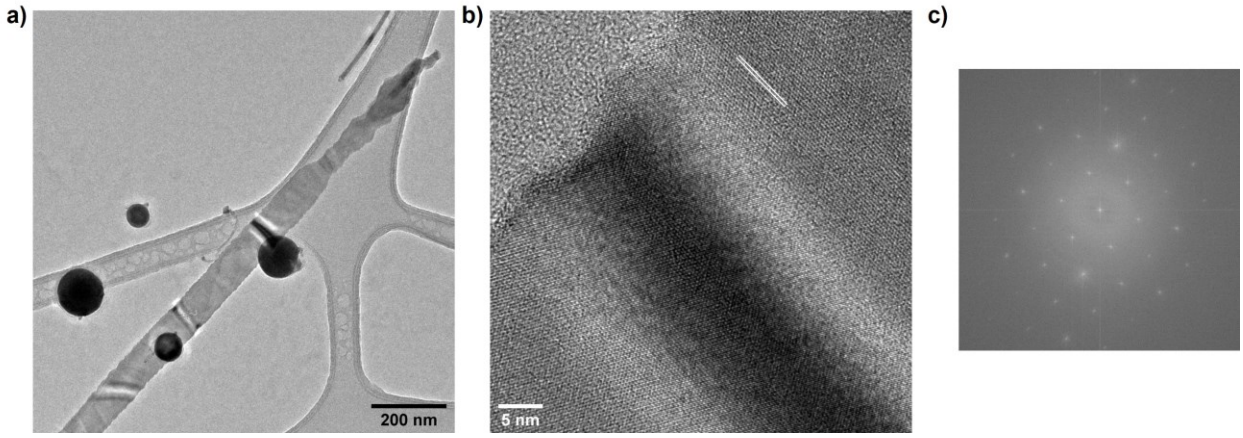

Figure S2. TEM image of a nanoribbon **(a)** with a lower magnification image **(b)** showing a continuous InP zinc blende lattice and a stripe pattern from buckling of the nanoribbon. The white lines highlight the 111 plane with a d spacing of 0.34 nm. **c)** The FFT of (b) confirms that the lattice is single crystalline.

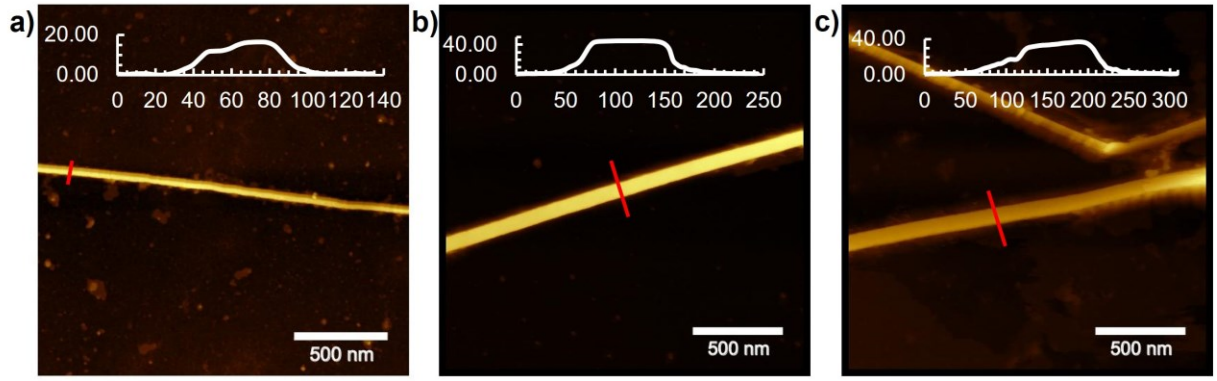

Figure S3. Additional AFM of InP NWs with inset graphs of the height profiles (height (nm) vs width (nm)) along the red line.

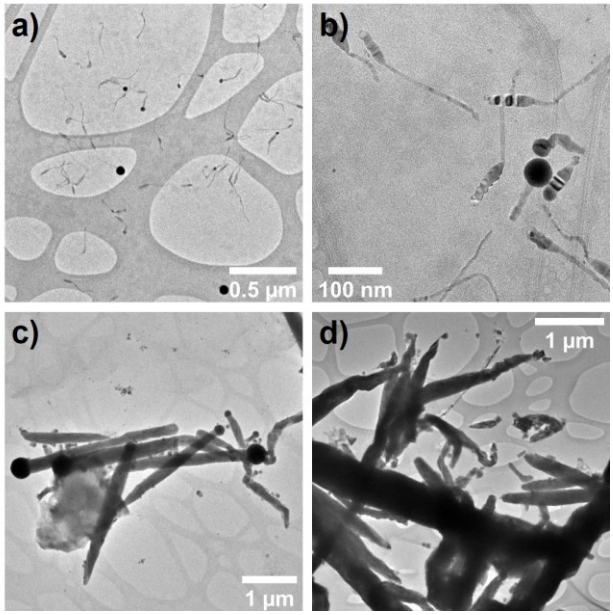

Figure S4. TEM images of NWs made using pre-made indium nanoparticles, one that uses indium nanoparticles in addition to $In(TFA)_3$ **(a,b)**, and the second that uses only pre-made indium nanoparticles as an indium source **(c,d)**.

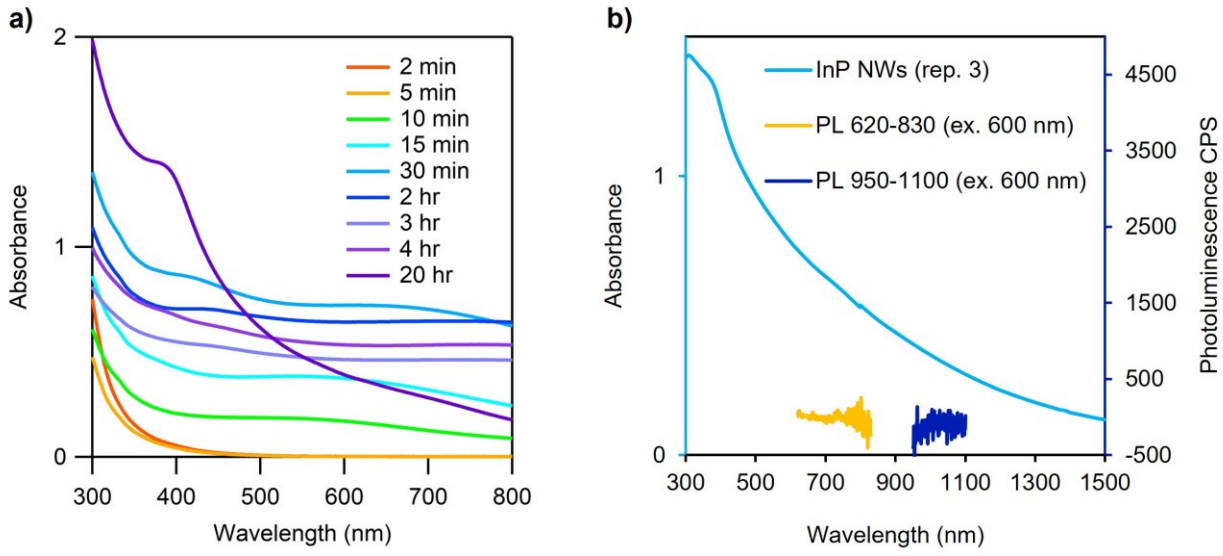

Figure S5. a) UV-vis absorbance spectra of aliquots taken over the course of the nanowire synthesis with 0 min at hot injection of the aminophosphine. **b)** UV-vis absorbance spectrum of purified InP nanowires from synthesis replicate 3 from 300 – 1500 nm, overlaid with photoluminescence spectra excited at 600 nm collected from 620 – 830 nm and 950 – 1100 nm. Collection between 830 and 950 is not feasible due to a detector crossover.

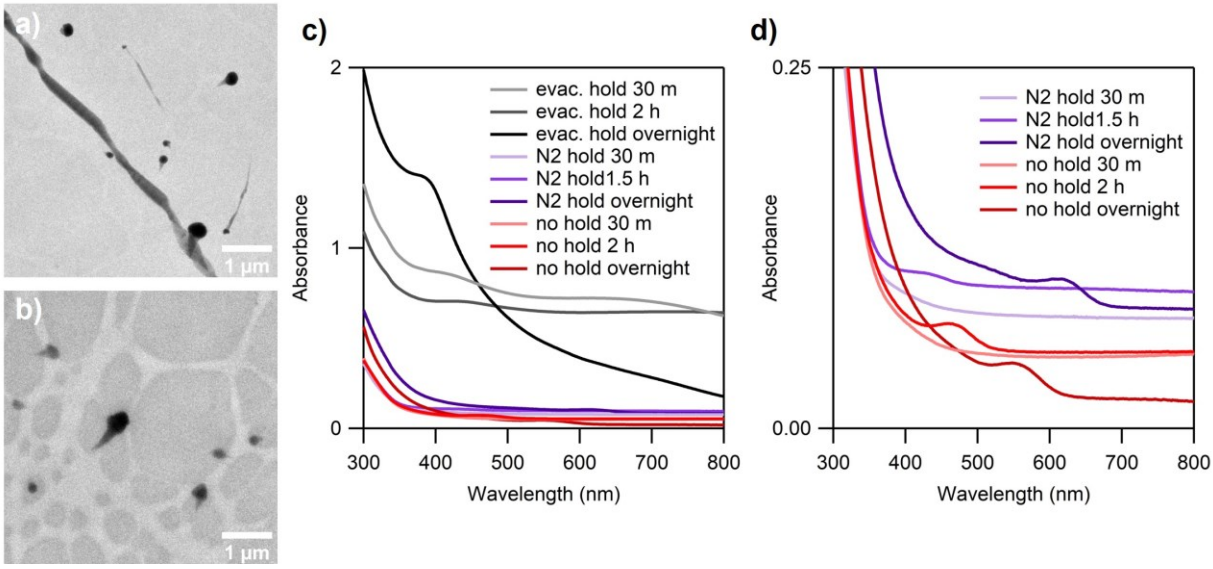

Figure S6. TEM images of products from control syntheses with an hour long hold at 120 °C under nitrogen **(a)** and skipping the evacuation step at 120 °C **(b)**. **c)** UV-visible absorbance spectra comparing the standard NW synthesis conditions (with an hour long evacuation step at 120 °C) to the two control syntheses. **d)** UV-visible absorbance spectra of the two control syntheses showing growth of quantum dot product primarily and overall low semiconductor absorbance.

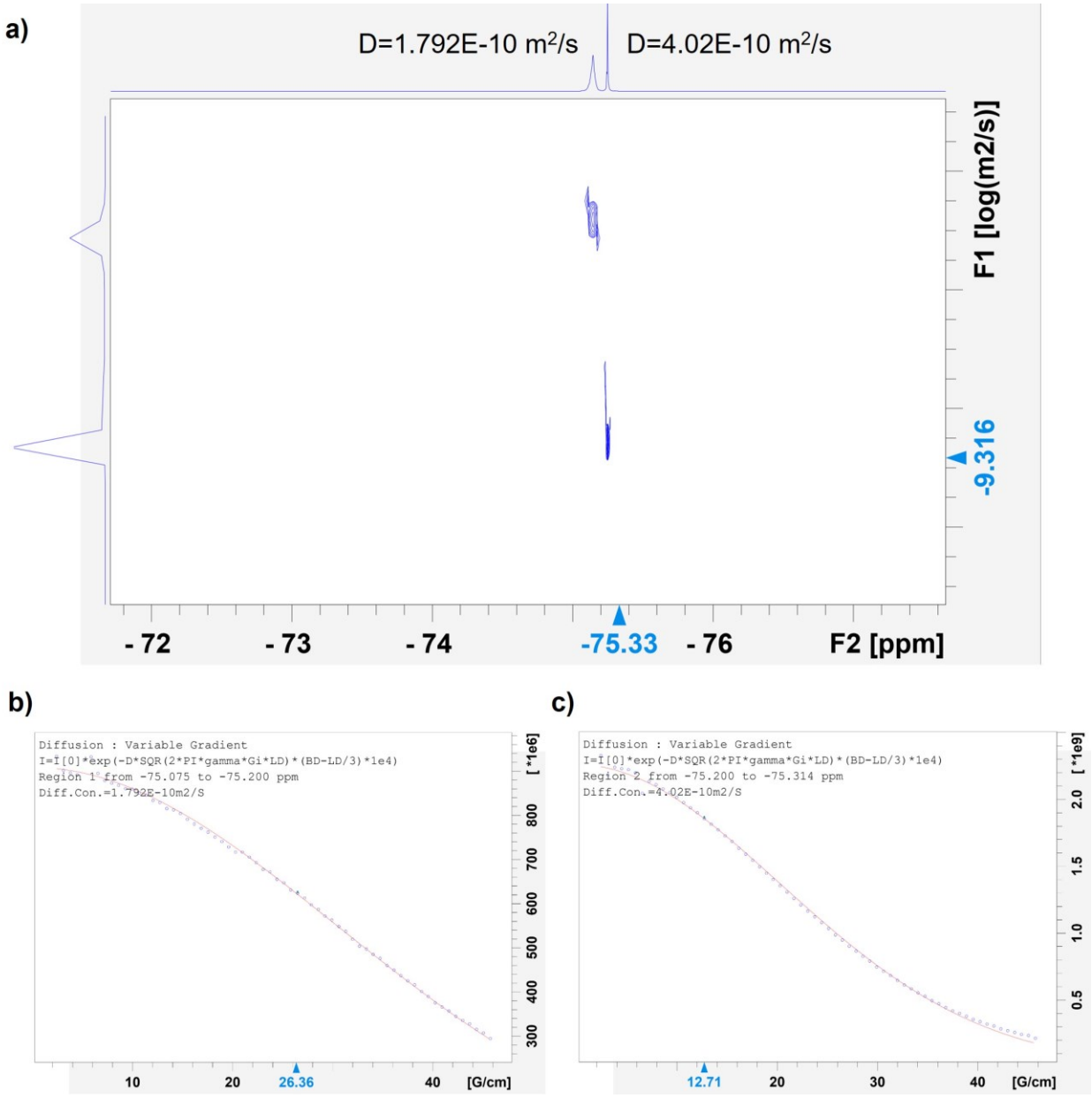
a)
D=1.792E-10 m²/s
D=4.02E-10 m²/s
F1 [log(m2/s)]
-9.316
- 72
- 73
- 74
-75.33
- 76
F2 [ppm]
b)
Diffusion : Variable Gradient
I=I[0]*exp(-D*SQR(2*PI*gamma*Gi*LD)*(BD-LD/3)*1e4)
Region 1 from -75.075 to -75.200 ppm
Diff.Con.=1.792E-10m2/S
[*1e6]
800
700
600
500
400
300
10
20
26.36
40
[G/cm]
c)
Diffusion : Variable Gradient
I=I[0]*exp(-D*SQR(2*PI*gamma*Gi*LD)*(BD-LD/3)*1e4)
Region 2 from -75.200 to -75.314 ppm
Diff.Con.=4.02E-10m2/S
[*1e9]
2.0
1.5
1.0
0.5
12.71
20
30
40
[G/cm]

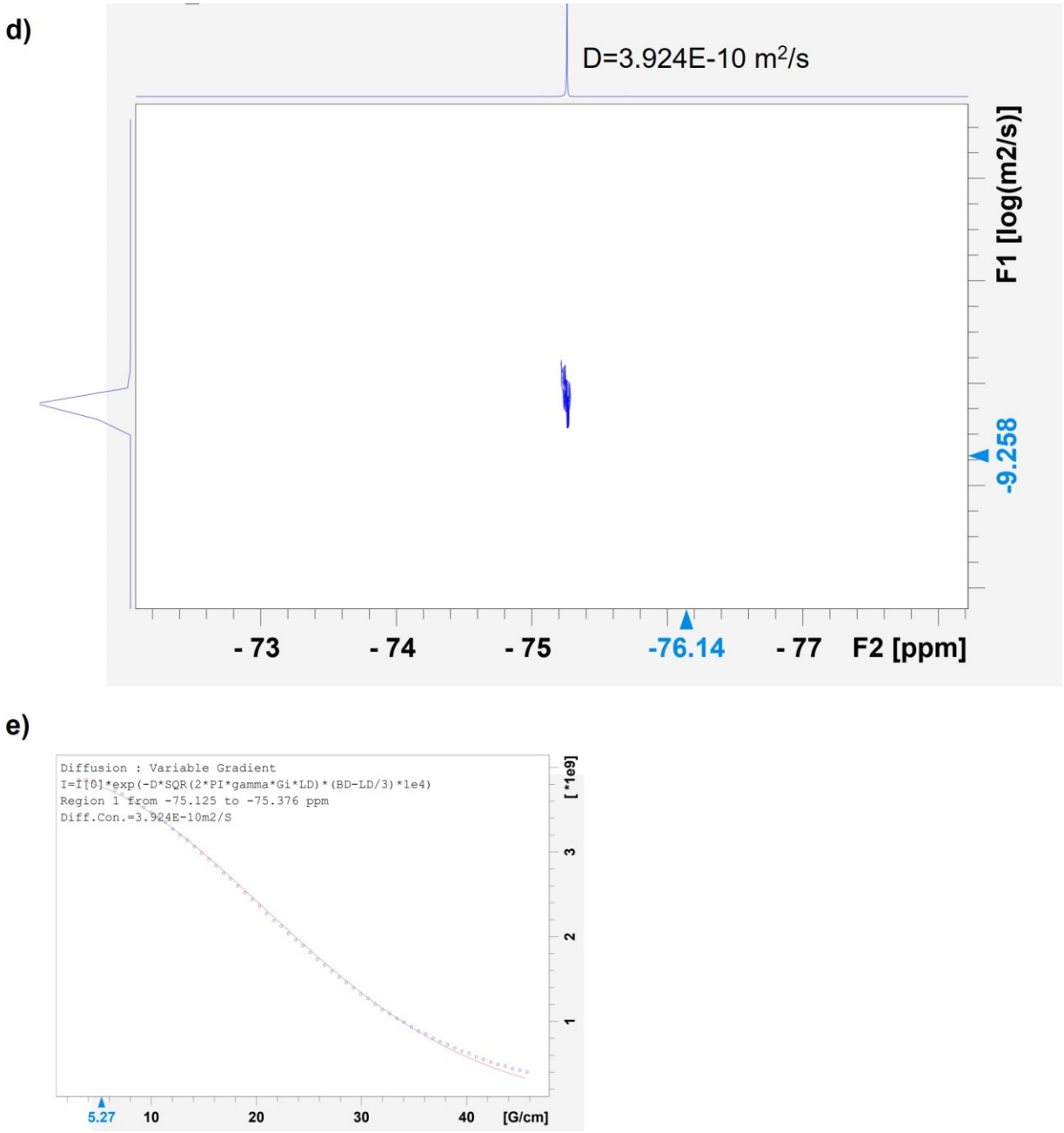

Figure S7. ^{19}F Diffusion-Ordered Spectra for aliquots taken **a)** at the beginning of the evacuation step at 120 °C with fits to extract the diffusion coefficients **(b, c)** and **d)** after one hour of evacuation at 120 °C with a fit to extract the diffusion coefficient **(e)**. The two peaks before the evacuation step, one broader and with a lower diffusion coefficient than the other suggest that the indium-trifluoroacetate complex exists in two forms, one more soluble than the other. Then, after the evacuation step is complete, only the sharper, higher diffusion coefficient peak remains implying that this step improves the solubility of the indium-trifluoroacetate complex.

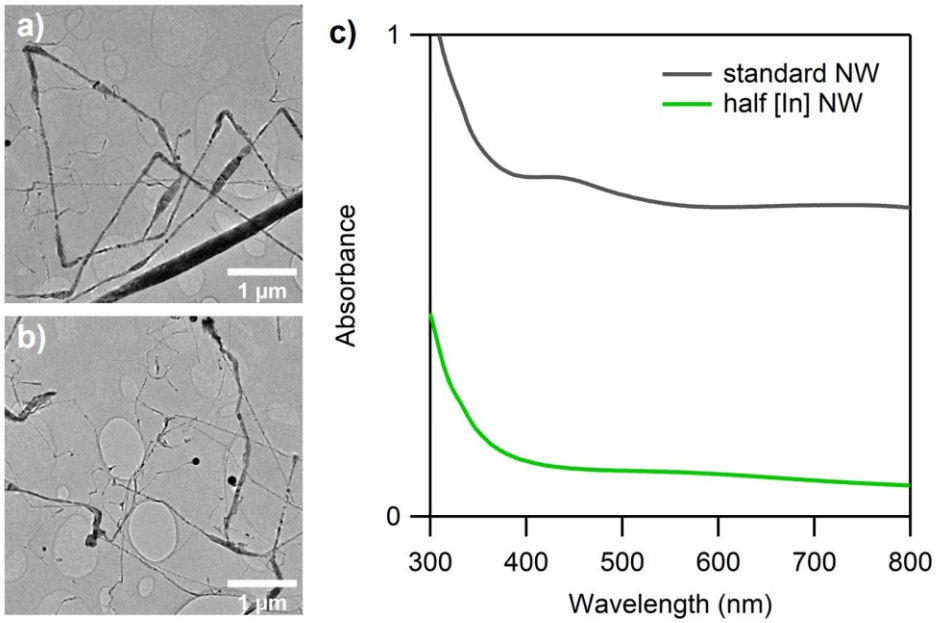

Figure S8. TEM of diameter dispersity increases with lower precursor concentration ([In]=0.03 M). **a)**, **b)** TEM images showing large InP nanowires present as well as smaller expected nanowires, with overall average diameter measured as 37.1 ± 42.5 nm. **c)** UV-visible absorbance spectra comparing the standard nanowire synthesis (at 2 hr) to the lower precursor concentration condition (1 hr).

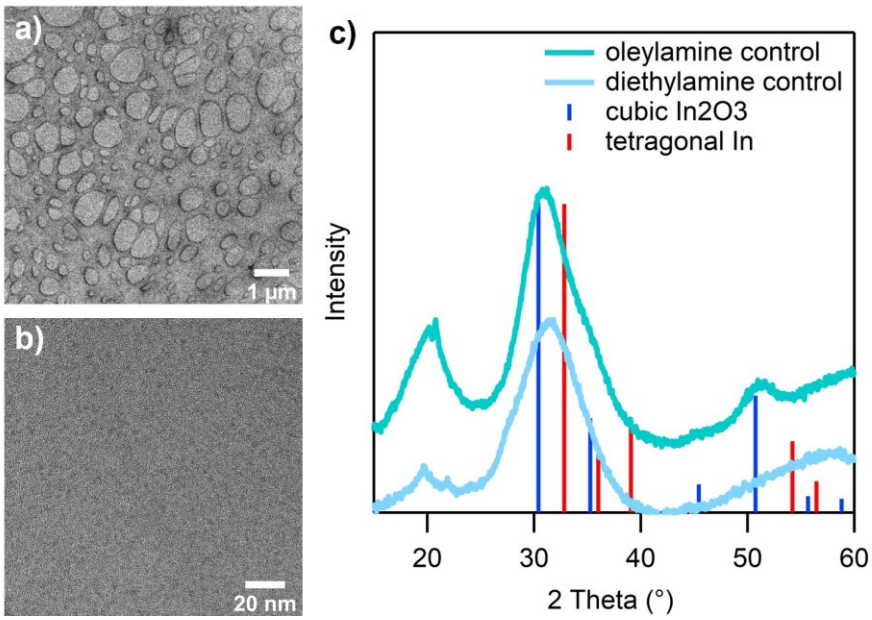

Figure S9. Low **(a)** and high **(b)** magnification TEM images of $In(TFA)_3$ in oleylamine after a 1 hour hold under vacuum at 120 °C and heating to 180 °C. **c)** Powder XRD patterns of purified nanoparticles resulting from the reaction of $In(TFA)_3$ in oleylamine and the reaction of In(TFA)3 in diethylamine and oleylamine.

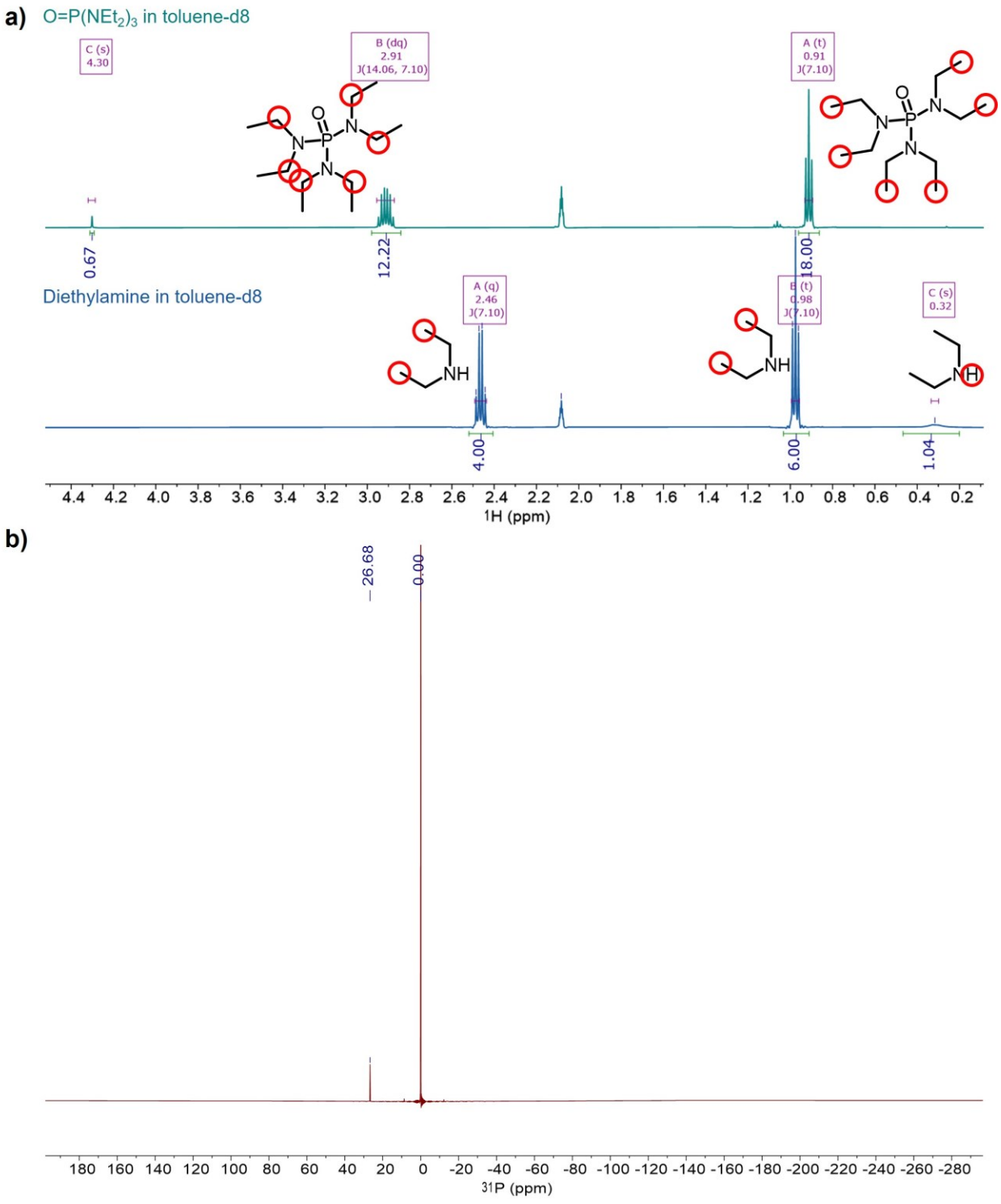

Figure S10. a) ^{1}H NMR spectra of purified O=P(NEt$_2$)$_3$ and diethylamine (500 MHz, toluene-d_8, DS 2, NS 10, D1 10 s). **b)** ^{31}P {H} NMR spectrum of purified O=P(NEt$_2$)$_3$ with an 80 weight % H_3PO_4 standard capillary (202 MHz, toluene-d_8, DS 2, NS 40, D1 10 s). Tris(diethylamino)phosphine has a chemical shift at 118 ppm.[12] Tris(dimethylamino)phosphine oxide (also known as hexamethylphosphoramide) has a chemical shift at 20.6 ppm in $CDCl_3$.[7]

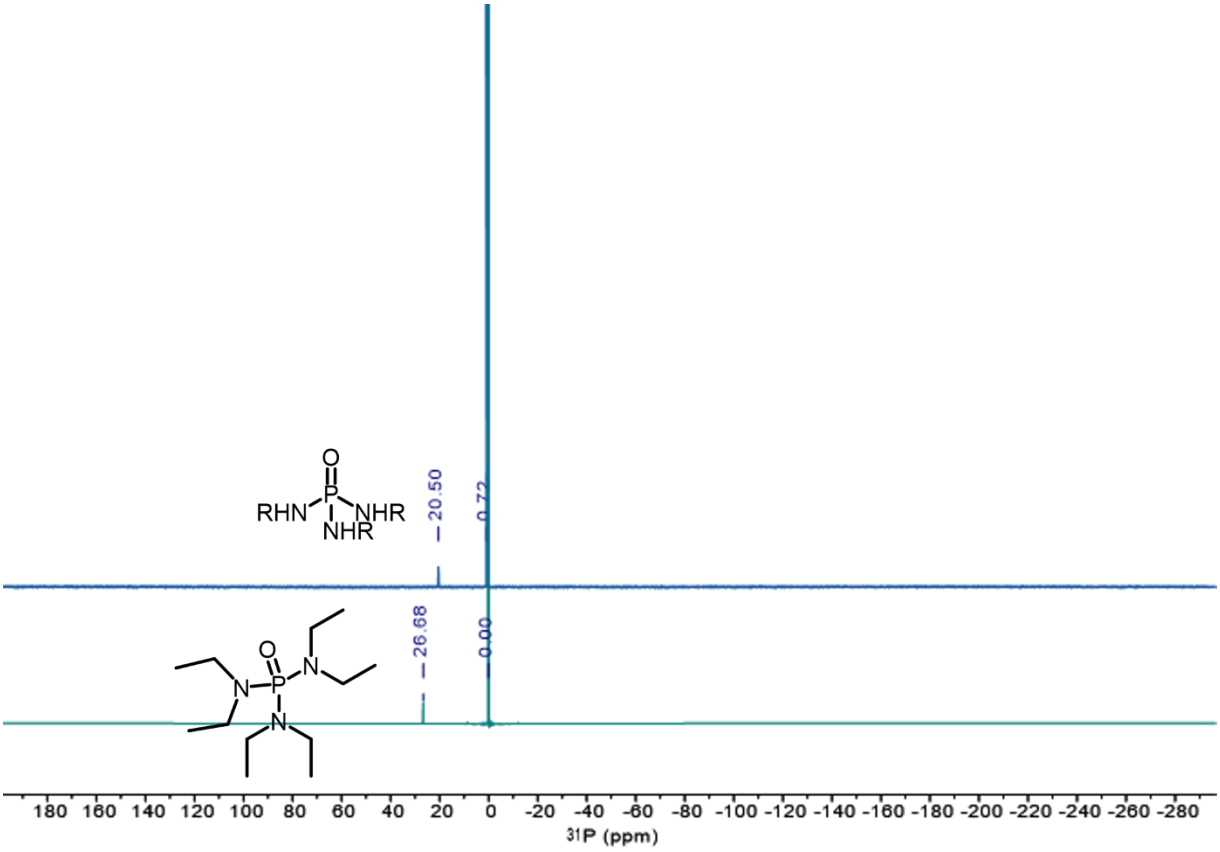
RHN
NHR
NHR
O
P
20.50
0.72
26.68
0.00
180 160 140 120 100 80 60 40 20 0 -20 -40 -60 -80 -100 -120 -140 -160 -180 -200 -220 -240 -260 -280
31P (ppm)

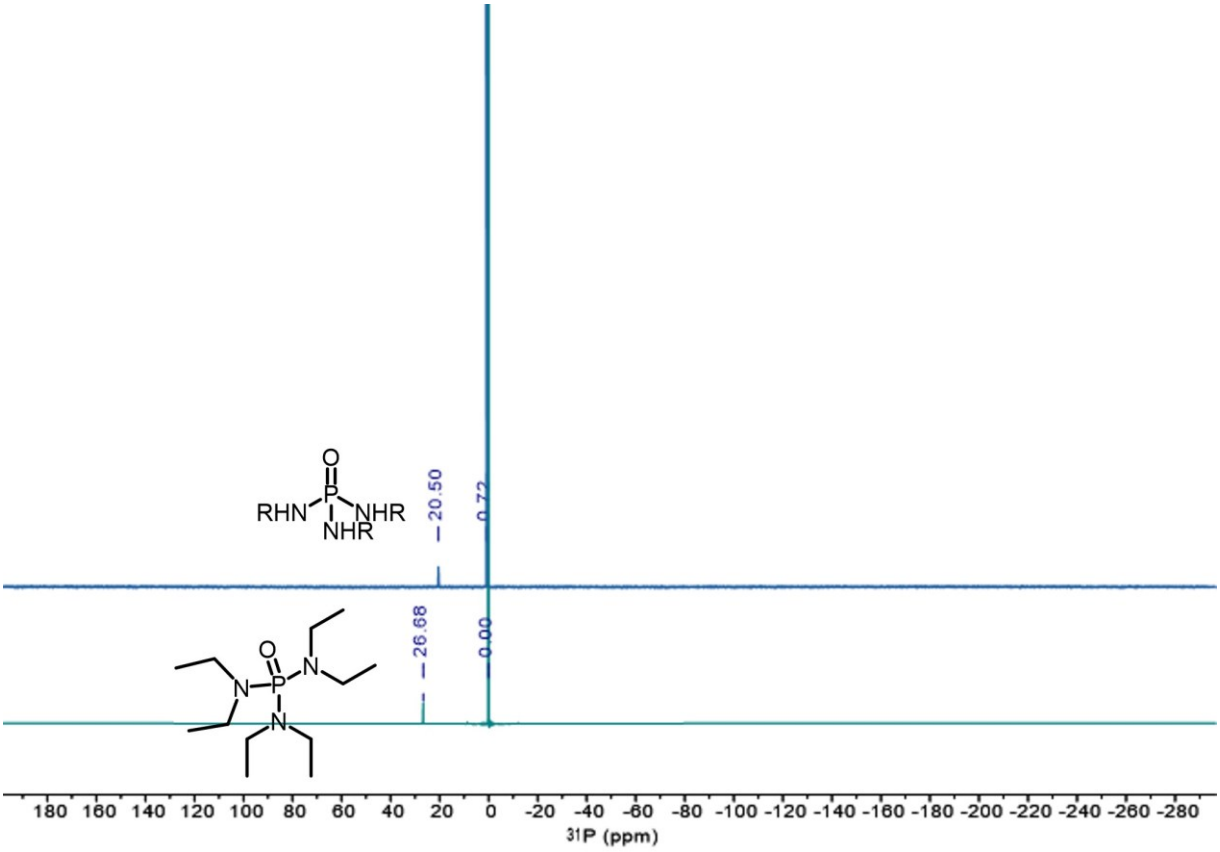
RHN
NHR
NHR
O
P
20.50
0.72
26.68
0.00
180 160 140 120 100 80 60 40 20 0 -20 -40 -60 -80 -100 -120 -140 -160 -180 -200 -220 -240 -260 -280
31P (ppm)

Figure S11. ^{31}P NMR spectrum of transaminated O=P(NHR)$_3$ (dark blue) with an 2 weight % H_3PO_4 standard capillary which has a shift of 0.72 ppm vs an 80 weight % H_3PO_4 standard, compared to the ^{31}P NMR spectrum of purified O=P(NEt$_2$)$_3$ (lighter blue) with an 80 weight % H_3PO_4 standard capillary (202 MHz, toluene-d_8, DS 2, NS 40, D1 10 s). R= $C_{18}H_{35}$.

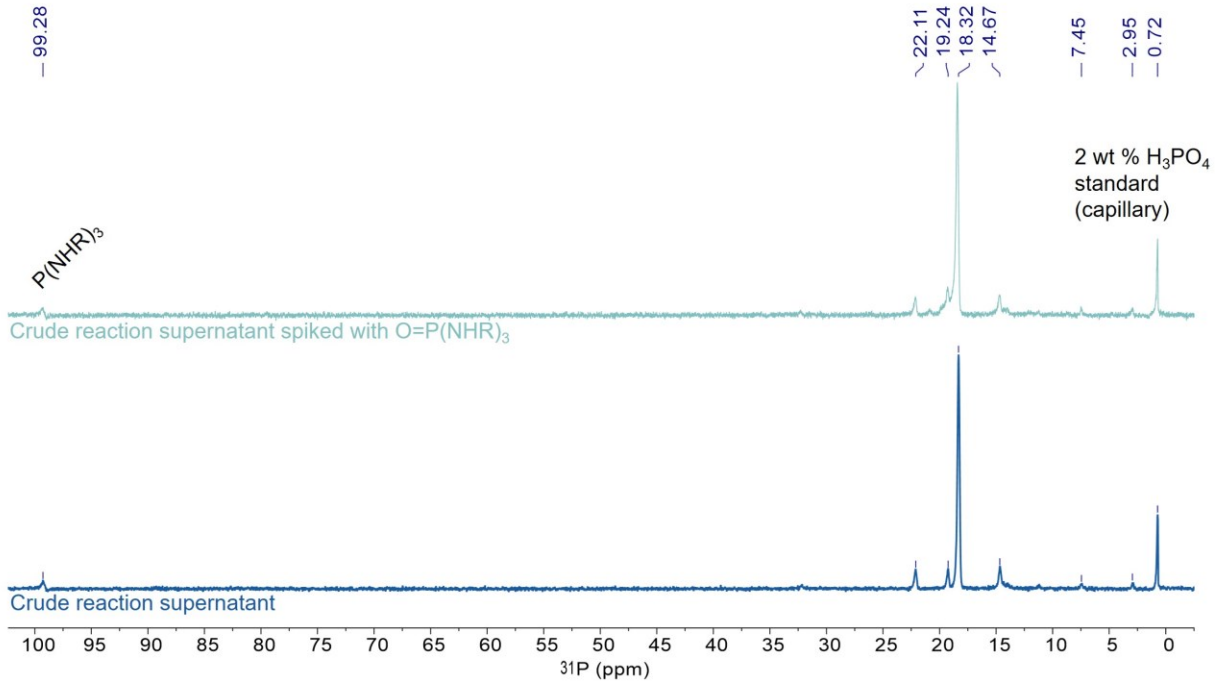

Figure S12. ^{31}P NMR spectrum of the crude nanowire reaction solution compared with the ^{31}P NMR spectrum of the same sample spiked with separately synthesized tris(oleylamino)phosphine oxide. The spectra are referenced to the peak at 0.72 ppm which is a 2 wt % H_3PO_4 standard, added as a sealed capillary. (202 MHz, toluene-d_8, DS 2, NS 40, D1 10 s)

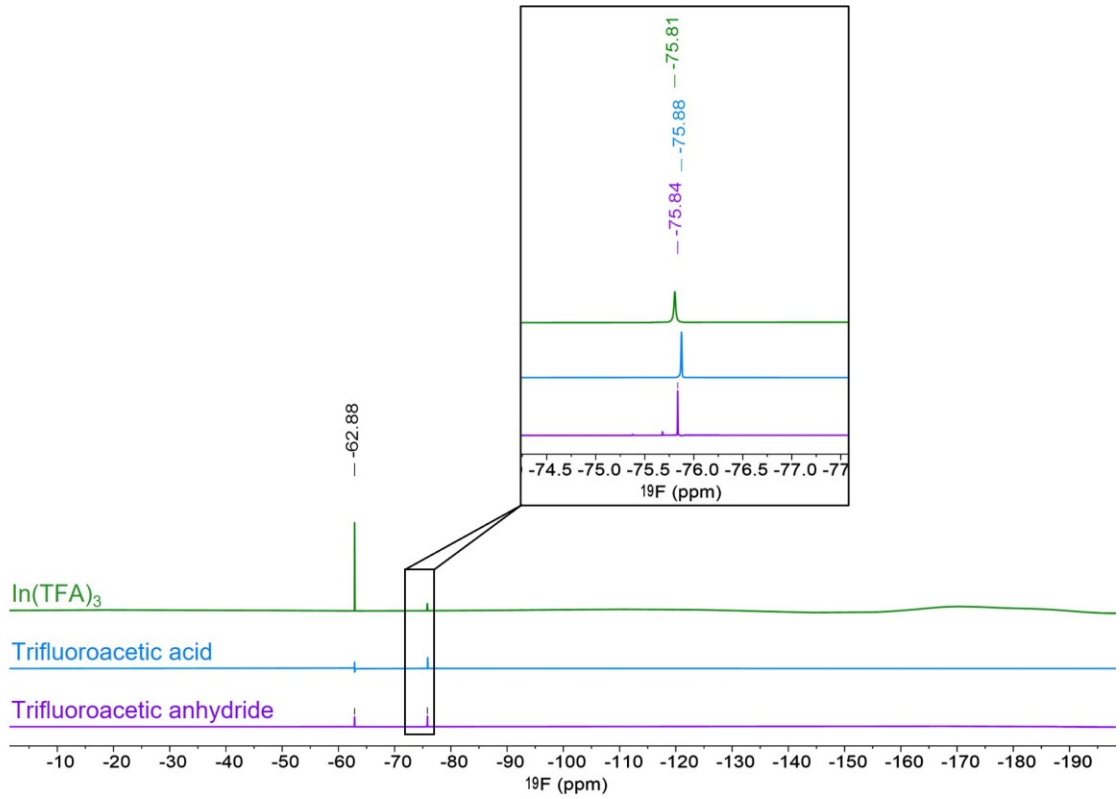

Figure S13. ^{1}H NMR spectra of In(TFA)$_3$, trifluoroacetic acid, and trifluoroacetic anhydride in oleylamine. (470 MHz, toluene-d_8, DS 2, NS 40, D1 10 s)

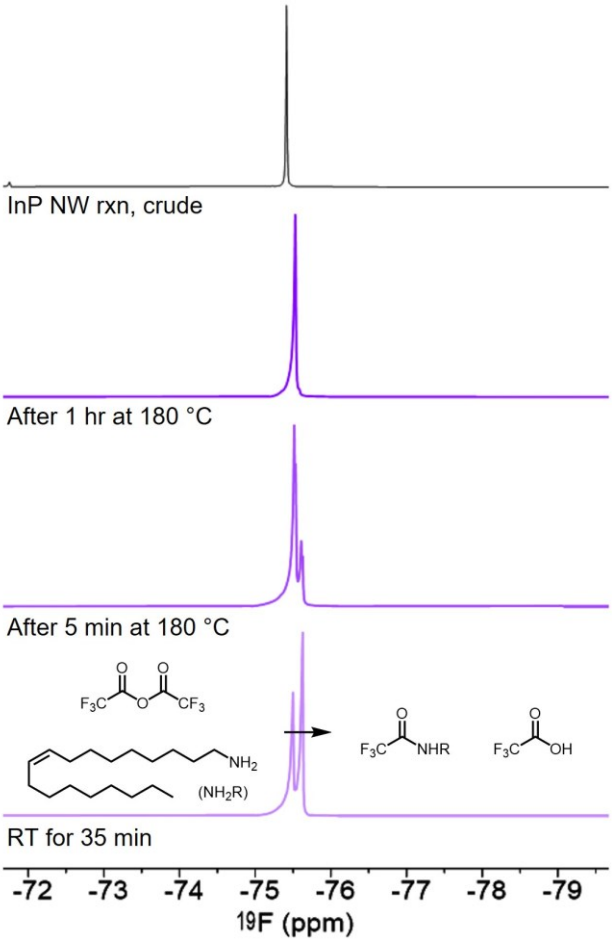

Figure S14. ^{19}F NMR spectra of (top) the crude nanowire reaction solution compared to aliquots of a control reaction between trifluoroacetic anhydride and oleylamine hypothesized to produce *N*-oleyltrifluoroacetamide. Trifluorotoluene was added as a reference. (470 MHz, toluene-d_8, DS 2, NS 40, D1 10 s)

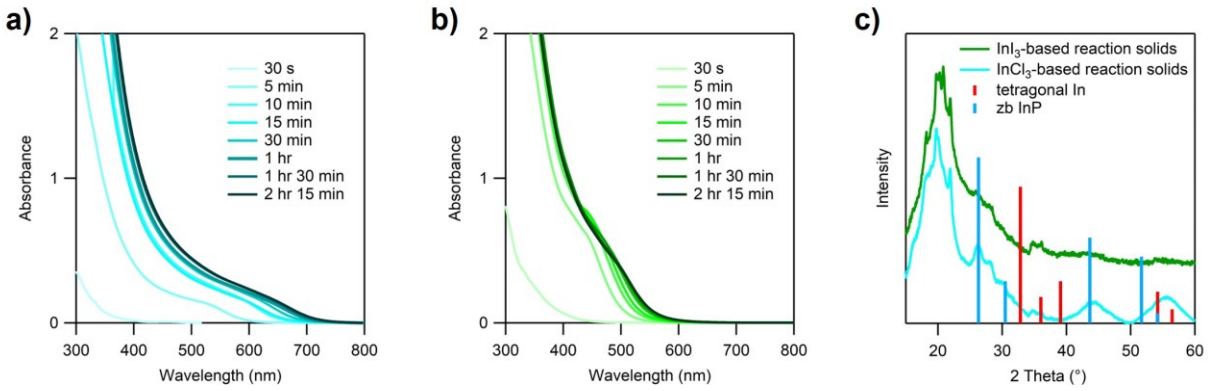

Figure S15. UV-vis absorbance spectra of aliquots from control syntheses using **a)** $InCl_3$ or **b)** InI_3. **c)** Powder X-ray diffraction patterns of the colloidally unstable fractions of both these controls to illustrate there are no InP nanowires or indium metal present.

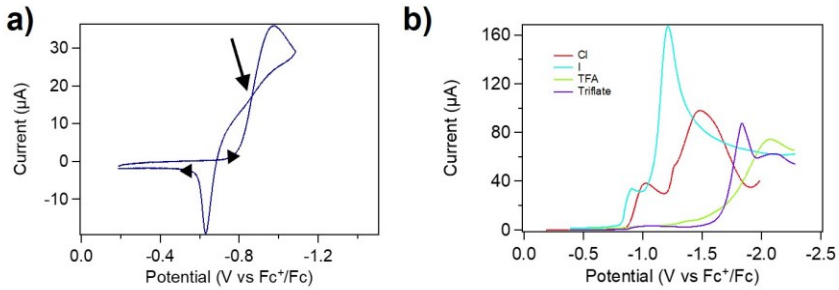

Figure S16. a) Cyclic voltammogram of $InCl_3$ with an arrow marking the inflection point of the indium nucleation loop reduction event. **b)** Cyclic voltammograms of the reduction events of the indium(III) salts of iodide, chloride, trifluoromethanesulfonate, and trifluoroacetate. Note how the reduction of the indium halide salts is more facile than the indium(III) trifluoromethanesulfonate or trifluoroacetate. (10 mL MeCN, 0.1 M $TBAPF_6$, glassy carbon WE, Pt wire CE, Ag pseudo reference electrode, in N_2 glovebox)

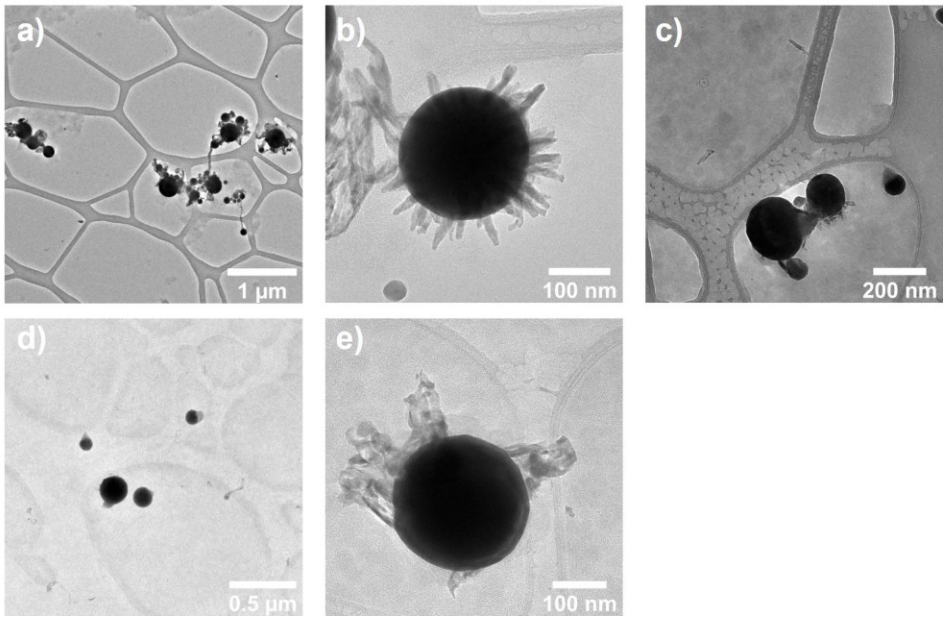

Figure S17. TEM images of multipod products formed when **(a,b)** the $In(TFA)_3$ is not pure, **(c)** 0.1 equivalent of trifluoroacetic acid is added, and **(d,e)** the reaction is P starved.

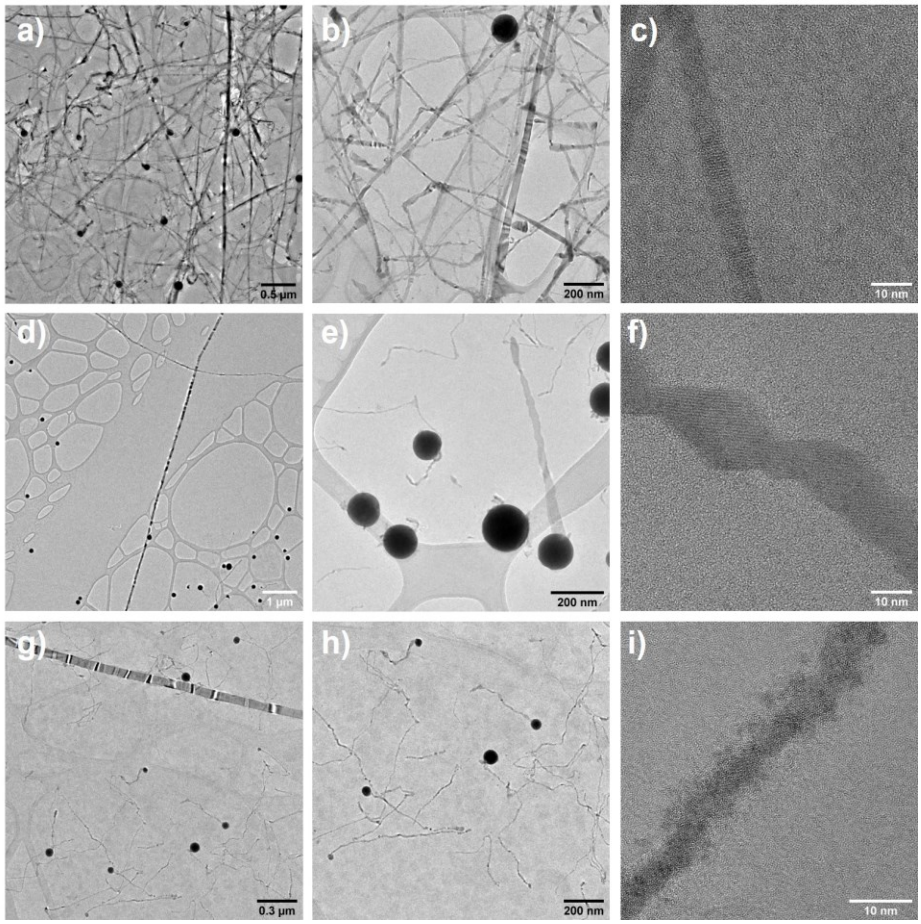
a)
0.5 µm
b)
200 nm
c)
10 nm
d)
1 µm
e)
200 nm
f)
10 nm
g)
0.3 µm
h)
200 nm
i)
10 nm

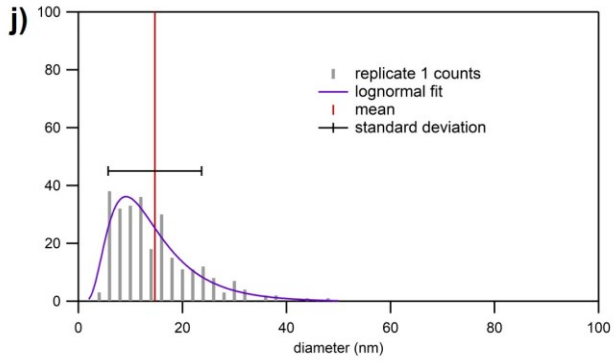
j)
replicate 1 counts
lognormal fit
mean
standard deviation
diameter (nm)

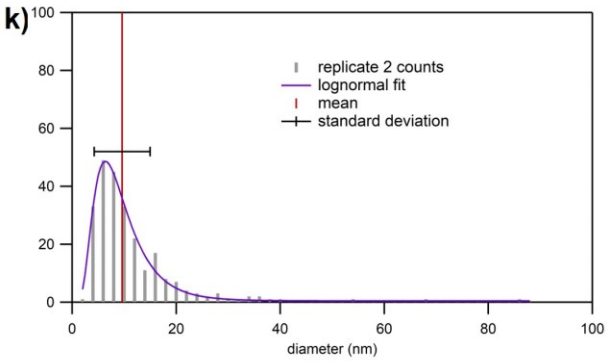
k)
replicate 2 counts
lognormal fit
mean
standard deviation
diameter (nm)

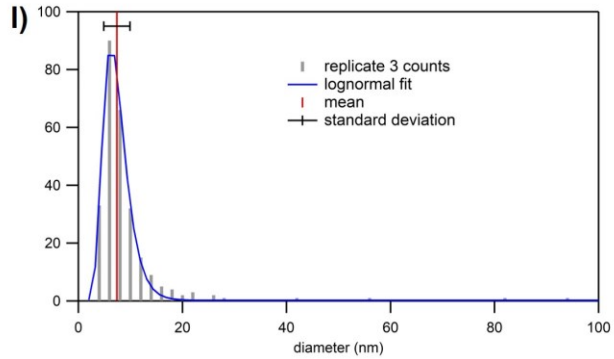
l)
replicate 3 counts
lognormal fit
mean
standard deviation
diameter (nm)

Figure S18. Additional TEM images showing reproducibility over three replicate InP nanowire syntheses **(1:a-c, 2:d-f, and 3:g-i)**. The nanowire diameter distribution is described well with a lognormal distribution, giving mean diameters of **(j)** 14.7 ± 9.0, **(k)** 9.6 ± 5.4, and **(l)** 7.4 ± 2.5 nm.

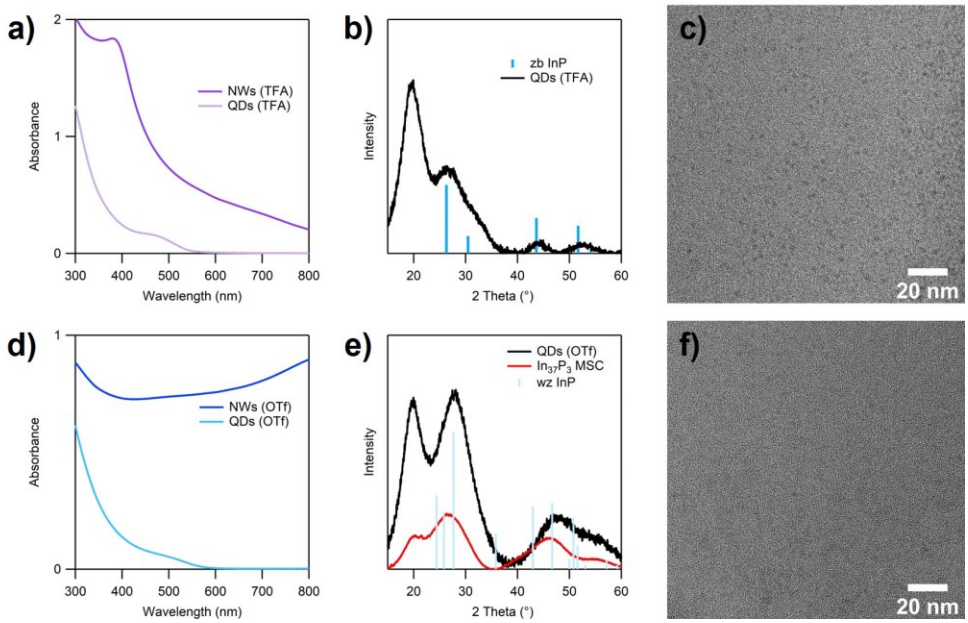

Figure S19. Characterization of InP QDs made using $In(TFA)_3$ including **(a)** UV-vis absorbance spectra deconvoluting the QD product from the NW product, **(b)** a pXRD pattern revealing zinc blende InP QDs with a crystallite size of 2.2 ± 0.9 nm, and **(c)** a TEM image of representative QDs. Characterization of InP QDs made using $In(OTf)_3$ including **(d)** UV-vis absorbance spectra deconvoluting the QD product from the NW product, **(e)** a pXRD pattern revealing small quasi-wurtzite InP QDs compared to the quasi-wurtzite $In_{37}P_{20}$ MSC pattern, and **(f)** a TEM image of representative QDs.

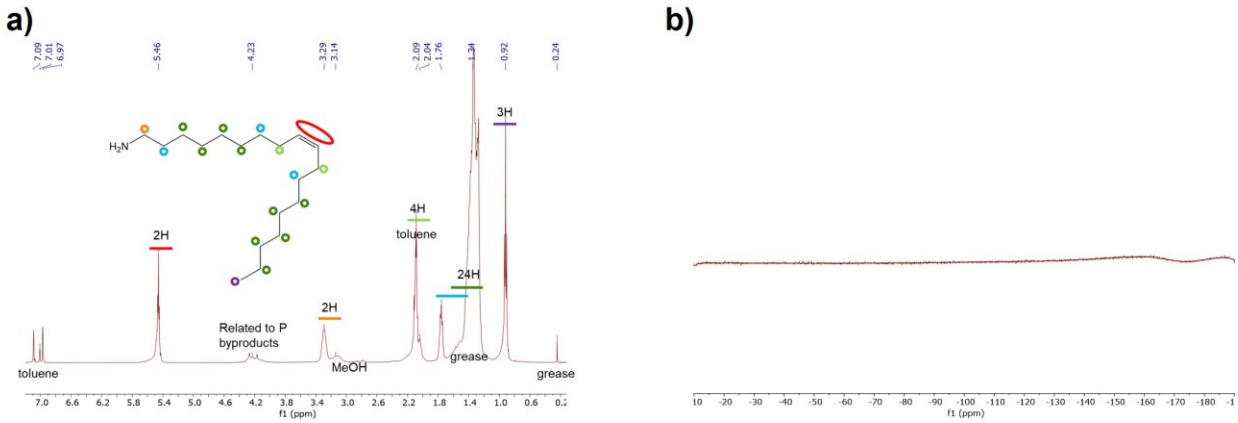

Figure S20. a) ^{1}H NMR spectrum of InP QDs made using $In(OTf)_3$ showing oleylamine both bound and free in the QD solution (500 MHz, toluene-d_8, DS 2, NS 10, D1 30 s). **b)** ^{19}F NMR spectrum of purified InP QDs made using $In(OTf)_3$ showing no triflate signal, suggesting there is no triflate found on the surface of the QDs after purification (470 MHz, toluene-d_8, DS 2, NS 40, D1 10 s).

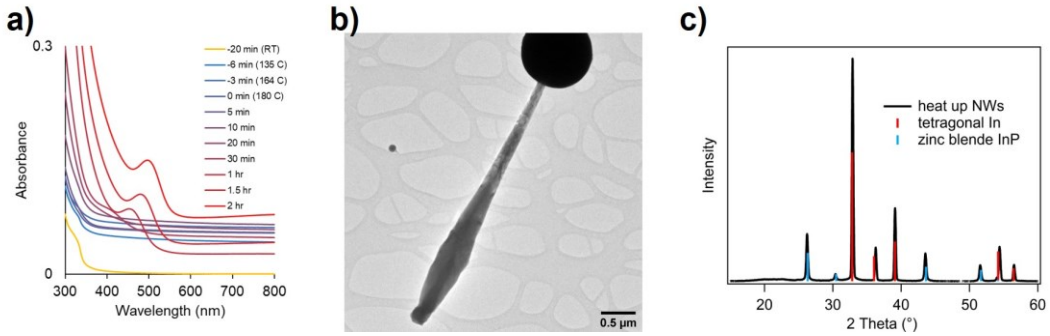

Figure S21. Characterization from the heat-up nanowire synthesis from $In(TFA)_3$ and $P(NEt_2)_3$ including **a)** UV-vis absorbance spectra of aliquots throughout the reaction with 0 minutes when the reaction temperature was achieved; **b)** TEM image showing an InP nanowire with an indium particle attached; **c)** pXRD pattern of the reaction product revealing bulk-like zinc blende InP and tetragonal indium metal.

3. References

(1) Pangborn, A. B.; Giardello, M. A.; Grubbs, R. H.; Rosen, R. K.; Timmers, F. J. Safe and Convenient Procedure for Solvent Purification. *Organometallics* **1996**, *15* (5), 1518–1520. https://doi.org/10.1021/om9503712.

(2) Sartori, P.; Fazekas, J.; Schnackers, J. Wasserfreie trifluoracetate der hauptgruppe III. *Journal of Fluorine Chemistry* **1972**, *1* (4), 463–471. https://doi.org/10.1016/S0022-1139(00)82967-X.

(3) Buffard, A.; Dreyfuss, S.; Nadal, B.; Heuclin, H.; Xu, X.; Patriarche, G.; Mézailles, N.; Dubertret, B. Mechanistic Insight and Optimization of InP Nanocrystals Synthesized with Aminophosphines. *Chem. Mater.* **2016**, *28* (16), 5925–5934. https://doi.org/10.1021/acs.chemmater.6b02456.

(4) Dreyfuss, S.; Pradel, C.; Vendier, L.; Mallet-Ladeira, S.; Mézailles, N. The Role of Water in the Synthesis of Indium Nanoparticles. *Chem. Commun.* **2016**, *52* (99), 14250–14253. https://doi.org/10.1039/C6CC08049A.

(5) Lim, T. H.; Ingham, B.; Kamarudin, K. H.; Etchegoin, P. G.; Tilley, R. D. Solution Synthesis of Monodisperse Indium Nanoparticles and Highly Faceted Indium Polyhedra. *Crystal Growth & Design* **2010**, *10* (9), 3854–3858. https://doi.org/10.1021/cg100857y.

(6) Wang, F.; Buhro, W. E. Role of Precursor-Conversion Chemistry in the Crystal-Phase Control of Catalytically Grown Colloidal Semiconductor Quantum Wires. *ACS Nano* **2017**, *11* (12), 12526–12535. https://doi.org/10.1021/acsnano.7b06639.

(7) B. Pavankumar, B.; Veerashekhar Goud, E.; Selvakumar, R.; Ashok Kumar, S. K.; Sivaramakrishna, A.; Vijayakrishna, K.; Brahmananda Rao, C. V. S.; N. Sabharwal, K.; C. Jha, P. Function of Substituents in Coordination Behaviour, Thermolysis and Ligand Crossover Reactions of Phosphine Oxides. *RSC Advances* **2015**, *5* (7), 4727–4736. https://doi.org/10.1039/C4RA13645D.
(8) Rachkov, A. G.; Schimpf, A. M. Colloidal Synthesis of Tunable Copper Phosphide Nanocrystals. *Chem. Mater.* **2021**, *33* (4), 1394–1406. https://doi.org/10.1021/acs.chemmater.0c04460.
(9) Dümbgen, K. C.; Leemans, J.; De Roo, V.; Minjauw, M.; Detavernier, C.; Hens, Z. Surface Chemistry of InP Quantum Dots, Amine–Halide Co-Passivation, and Binding of Z-Type Ligands. *Chem. Mater.* **2023**. https://doi.org/10.1021/acs.chemmater.2c02960.
(10) Larson, H.; Cossairt, B. M. Indium–Poly(Carboxylic Acid) Ligand Interactions Modify InP Quantum Dot Nucleation and Growth. *Chem. Mater.* **2023**, *35* (15), 6152–6160. https://doi.org/10.1021/acs.chemmater.3c01309.
(11) Rosenau, C. P.; Jelier, B. J.; Gossert, A. D.; Togni, A. Exposing the Origins of Irreproducibility in Fluorine NMR Spectroscopy. *Angewandte Chemie International Edition* **2018**, *57* (30), 9528–9533. https://doi.org/10.1002/anie.201802620.
(12) Tessier, M. D.; De Nolf, K.; Dupont, D.; Sinnaeve, D.; De Roo, J.; Hens, Z. Aminophosphines: A Double Role in the Synthesis of Colloidal Indium Phosphide Quantum Dots. *J. Am. Chem. Soc.* **2016**, *138* (18), 5923–5929. https://doi.org/10.1021/jacs.6b01254.